Tellus (1993), 45B, 145–159
Printed in Belgium – all rights reserved

TELLUS
ISSN 0280–6509

Size distribution of Antarctic submicron aerosols

By TOMOYUKI ITO, *Ozone Layer Monitoring Office, Observations Department, Japan Meteorological Agency, 1-3-4 Ohte-Machi, Chiyoda-Ku, Tokyo 100, Japan*

(Manuscript received 27 August 1991; in final form 3 June 1992)

ABSTRACT

The method and results of the observation of the size distribution of submicron aerosols carried out at Syowa station (69°00′S, 39°35′E) in the sunlit months from August to December in 1978 are described. The most important finding in this series of observations is that the bimodal size distribution with a trough at around 10^{-6} cm in radius is seen in almost all observations. The prevalence of the bimodal size distribution observed at Syowa station in the sunlit months gives evidence of new particle formation in the Antarctic troposphere. Based on simplified theoretical calculations, it is concluded that the production rate of new particles is about 4×10^{-4} cm^{-3} s^{-1} in the summer in Antarctica which for instance could be yielded by homogeneous conversion of an SO_2 concentration of 1 μg m^{-3} at a rate of 0.5% hr^{-1}. The most plausible precursors of SO_2 involved in this process seem to be rather inert gases such as COS, CS_2, etc. DMS plays a small rôle in this new particle formation process, although it does play an important rôle in maintaining the aerosol mass concentration in the Antarctic atmosphere.

1. Introduction

Submicron aerosols in the troposphere obstruct incident solar radiation directed towards the earth's surface, and also prevent heat from escaping as infrared radiation from the earth to space. Hygroscopic particles in the troposphere act as absorbers of water vapor to cause degradation of atmospheric transparency of light, by increasing in their size with an increase in atmospheric relative humidity. Some aerosol particles can act as cloud condensation nuclei or as ice nuclei, on which water droplets or ice crystals are formed in the troposphere. The concentration of such nuclei is one of the controlling factors in determining the microstructure of clouds. It should be noted, however, that aerosol particles not only play a rôle in cloud-physical processes but also affect the atmospheric radiation budget by controlling the microstructure of clouds. Thus, the atmospheric submicron aerosols play important rôles in two atmospheric processes essential to meteorology, namely the radiation budget and the water circulation in the atmosphere.

In this paper, the atmosphere (troposphere) which is not directly affected by pollution from local anthropogenic sources is named the "background atmosphere". The background atmosphere covers most of the troposphere except for the boundary layer over continents with numerous anthropogenic sources of air pollution. Since the background atmosphere is characterized by its global extent and quite low aerosol concentration, slight changes in the properties and/or concentration of aerosol particles in the background atmosphere may cause large changes in the global atmospheric processes leading to a global climatic change (e.g., Charlson et al., 1987).

Antarctica is expected to have the cleanest air in the global atmosphere because it is located in the Southern Hemisphere which has a smaller land area and less human activities than the Northern Hemisphere. Air circulation over Antarctica also seems to prevent the direct transport of air originating in the lower latitudes through the lower troposphere. Therefore for studying background aerosols, Antarctica provides attractive sites free from the "noise" due to anthropogenic pollution.

The historical reviews of aerosol measurements in Antarctica are given by Hogan (1975), Shaw (1979) and Shaw (1988). The latter also gives an

extensive review on recent studies of the properties and behavior of Antarctic aerosols. The activities of air quality monitoring at the South Pole are reviewed by Robinson et al. (1988), which also includes aerosol monitoring.

Observations of submicron aerosols have been carried out at Syowa station (69°00′S, 39°35′E) since 1976. The most extensive year-round observation was carried out in 1978 followed by the aerosol observations using balloon sondes and an airplane in 1983 and 1984. The results of these observations have been reported elsewhere (Ito and Iwai, 1981; Ito, 1985, 1989). The most important finding through these studies was that the phenomena possibly related to photochemical production and/or growth of particles in the troposphere in and around Antarctica were appreciably seen in each observation.

As for the size distribution of submicron aerosols, the method of observation and discussion about the observational results were first given by Ito (1982) in Japanese and appeared in a publication of limited circulation. This paper aims to give a translation of Ito (1982) but also to extend the discussion about aerosol processes based on the recent knowledge of the background aerosols and precursor gases.

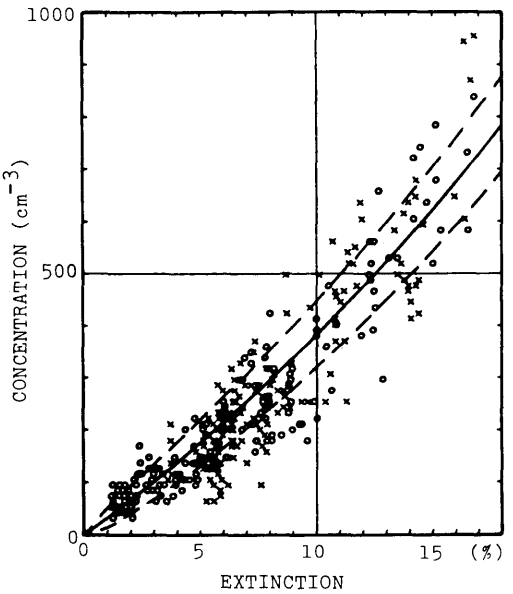

Fig. 1. In situ calibration of the Pollak counter. The solid curve is the calibration curve derived by the quadratic least square fit to the plotted individual comparisons. The two dashed curves indicate the expected standard deviation of measurements with the Aitken counter, assuming the statistical scattering of the Poisson distribution.

2. Instrument

The size distribution of "large particles" was measured with the optical particle counter which is similar in principle to the Royco light-scattering particle counter. Aerosol particles are assumed to be spherical in shape with the refractive index of 1.4 (Ito, 1985).

The instrument used for the measurement of size distribution of Aitken particles is the same one used in the previous work (Ito, 1980), which consists of two identical Pollak counters and four diffusion pipes.

Fig. 1 shows the in situ calibration of the Pollak counter, carried out at Syowa station by comparative measurements with a photographic recording Aitken counter (Ito, 1976). The scattering of the plotted data is statistical, due to the small sample size in the Aitken counter (the counting view volume is 0.1 cm^3) and not instability in the Pollak counter measurements. The solid curve in Fig. 1 is the calibration curve derived from a quadratic least square fit to the plotted individual comparisons. The dashed lines indicate the expected standard deviation of the concentration measured with the Aitken counter, assuming the statistical scattering of the Poisson distribution. The fact that the more than 60 % of the plotted data fall between the two dashed lines supports the above explanation on the cause of the scattering of the plotted data.

The diffusion pipe is a bundle of thin nickel tubes with an inside diameter of 2.0 mm and a length of 1.0 m, encased in a brass pipe 1.2 m long. The spaces between the tubes are filled with a plastic binding agent so that aerosols can only pass through the insides of the thin tubes. When aerosols flow through the narrow channels of the diffusion pipe, their concentration decays due to the Brownian diffusion of particles to the walls of the channels. The penetration is defined as the fraction of particles passing through the channels without being captured by the walls, and is expressed as a function of the particle radius (r) and traverse time (t) taken by air to pass through

the channel. A smaller particle size or a longer traversing time results in lower penetration. The penetration of polydisperse aerosols with the size distribution of $f(r)$ is expressed as

$$R(t) = \int_0^\infty f(r)\, P(r, t)\, \mathrm{d}r, \qquad (1)$$

where $P(r, t)$ is the penetration of monodisperse aerosol with the radius of r passing through the channel in a traverse time of t, and $R(t)$ is the penetration of polydisperse aerosols which is measured as a function of traverse time.

Fig. 2 represents an example of the time change of size distribution obtained from a series of penetration data measured every 30 min. The top diagram represents the original data; the series of dots indicates the total aerosol concentrations before entering the diffusion pipes and the six dash-dot lines represent the decayed concentrations after passing through the diffusion pipes. The bottom diagram represents the retrieved size distributions every 30 min.

In order to test the reliability of the size distribution obtained using the present method, the following numerical simulation was carried out. A set of penetrations for the six different traversing times was calculated for a given model size distribution with eq. (1), and assumed errors were added to those calculated penetrations to simulate the observational error. Then the size distribution was retrieved from the set of calculated penetrations which contained assumed errors. The resultant size distribution was compared with the original model size distribution.

The following model size distributions, for the radius range of $2 \times 10^{-7} < r < 2 \times 10^{-5}$ cm, were used in the simulation:

Model-I $\quad \mathrm{d}n/\mathrm{d}\log r = \sqrt{10},$

Model-II $\quad \mathrm{d}n/\mathrm{d}\log r = 10^3 \sqrt{5r},$

Model-III $\quad \mathrm{d}n/\mathrm{d}\log r = 10^{-2}/\sqrt{5r}.$

When the ordinate and the abscissa are taken as $\mathrm{d}n/\mathrm{d}\log r$ and r in a logarithmic scale, these size distributions are represented by straight lines crossing at the point ($r = 2 \times 10^{-6}$, $\mathrm{d}n/\mathrm{d}\log r =$

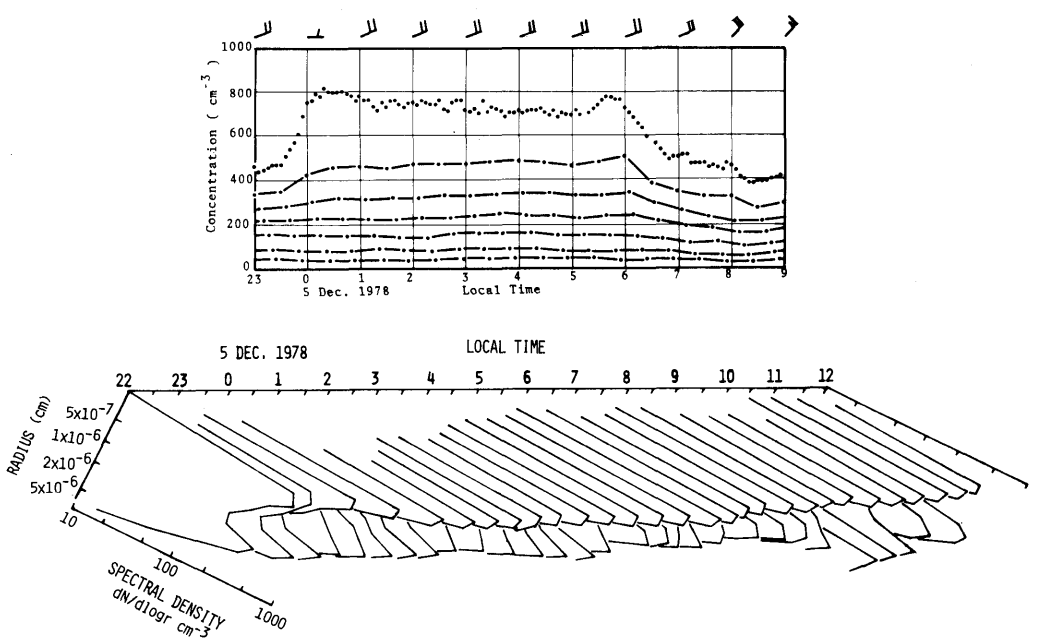

Fig. 2. An example of time change of size distribution obtained from a series of the penetration data measured every 30 min. In the top diagram, the series of dots indicates the total aerosol concentrations before entering the diffusion pipes and the six dash-dot lines represent the decayed concentrations after passing through the diffusion pipes. The bottom diagram represents the retrieved size distributions every 30 min.

$\sqrt{10}$) and have the gradients of 0, 0.5 and -0.5 for models I, II and III, respectively.

Fig. 3 shows the result of the simulation. The thin lines represent the model size distributions. The thick curves represent the size distributions obtained from the series of penetrations without assumed error. Even in the case without assumed error, the retrieved size distributions deviated erroneously from the original model distributions around both ends of the size range. This is due to the fact that the range of the traversing time applied, that is about 5 to 160 s, is not sufficiently wide. However, when the traversing time is shorter than 5 s, the ranway distance (the distance from the entrance of the channels before the steady flow has established) is so long that the theoretical penetration $P(r, t)$ is not applicable (Davies, 1973). On the other hand, when the traversing time is longer than 160 s, the effect of axial diffusion cannot be ignored in the theoretical derivation of $P(r, t)$ (Tan and Hsu, 1971). Thus, the range of the traversing time applied in the present instrumentation is close to the maximum available.

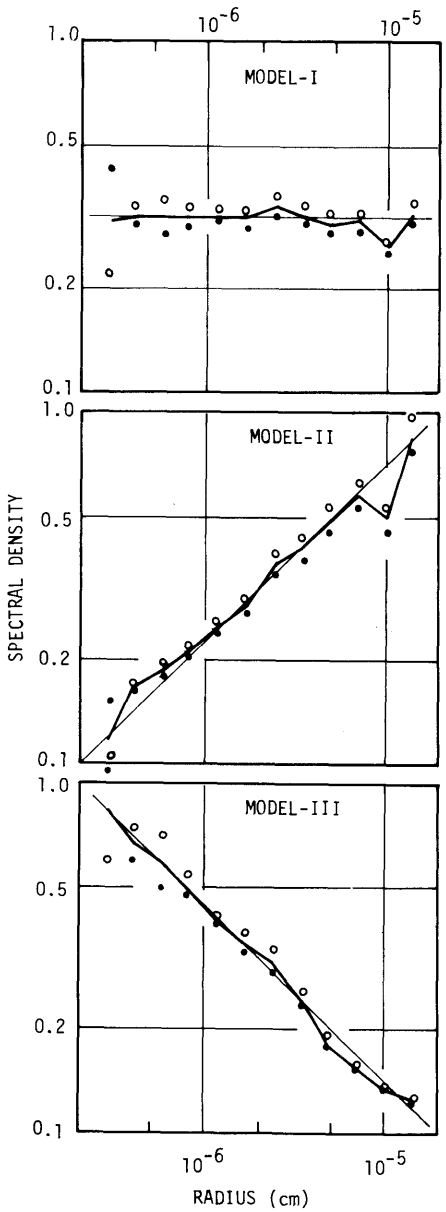

In Fig. 3, the size distributions retrieved from the penetrations with assumed errors are also shown. The series of closed (open) circles represents the size distribution obtained from the series of penetrations multiplied by factor 0.95 (or 1.05) to simulate the observational error of $\pm 5\%$. It is clear, however, that observational error within $\pm 5\%$ does not cause serious deformation of the retrieved size distribution compared with the original model distribution within the radius range between 4×10^{-7} and 7×10^{-6} cm.

The size distributions presented here, however, may be considered provisional because these have not been confirmed with other methods, although the arrangements for the measurement and retrieval procedure were done as carefully as possible in order to meet theoretical requirements.

Fig. 3. Simulation to test the reliability of the retrieval of size distribution from penetration data. The thin lines represent the model size distributions.

Model-I $\quad dn/d \log r = \sqrt{10}$

Model-II $\quad dn/d \log r = 10^3 \sqrt{5r}$

Model-III $\quad dn/d \log r = 10^{-2}/\sqrt{5r}$.

The thick curves represent the size distributions obtained from a series of penetrations calculated with eq. (1). The series of closed (open) circles represents the size distribution obtained from the series of penetrations multiplied by factor 0.95 (or 1.05) to simulate the observational error of $\pm 5\%$.

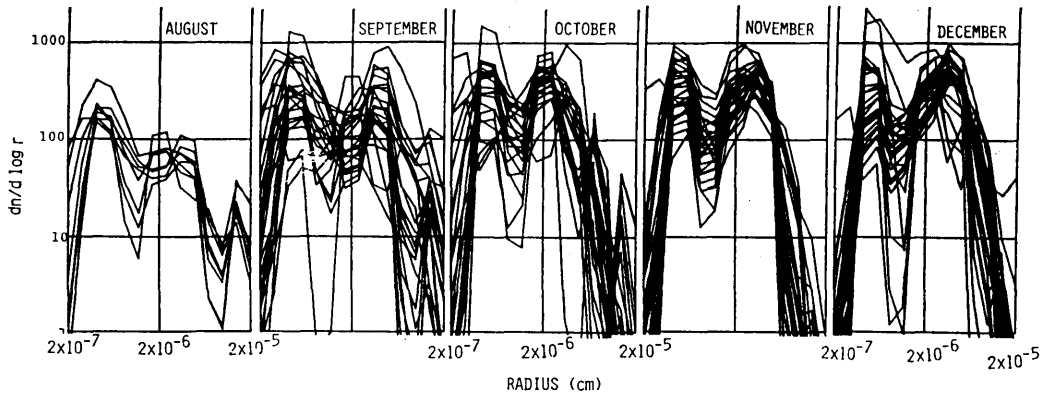

Fig. 4. Daily average size distributions of Aitken particles obtained each month from August to December in 1978 at Syowa station.

3. Results

Fig. 4 represents the superposition of daily average size distributions of Aitken particles obtained each month from August to December in 1978 at Syowa station. The data suspected to have contamination from local sources was rejected. The most notable point in the figure is that almost all size distributions were of bimodal shape with the trough around 10^{-6} cm in radii. The present result gives a striking contrast with the previous results obtained in the North Pacific where the same instrument and method were used. Most of the previous observations did not give bimodal size distributions (Ito, 1980). It is clear in Fig. 3 that the present bimodal shape is not created numerically by the procedure of retrieving the size distribution from the penetration data.

4. Discussion

4.1. Characteristics of the size distribution of submicron aerosols in the Antarctic troposphere

Characteristics of size distributions are more clearly seen when they are expressed in a form of surface area size distribution (S: $ds/d\log r$) and volume size distribution (V: $dv/d\log r$) as well as number size distribution (N: $dn/d\log r$). Fig. 5 which is reproduced from Ito (1985) represents the monthly average size distributions of Aitken and "large" particles in these three forms. For the reasons discussed in Ito (1985), the distribution of Aitken particles larger than 5×10^{-5} cm are ignored. Based on Fig. 5, submicron aerosols at Syowa station can be classified into three size categories. They are the radius subranges smaller than 10^{-6} cm, those between 10^{-6} and 10^{-5} cm and those larger than 10^{-5} cm.

Particles smaller than 10^{-6} cm in radius make up one mode of the bimodal number size distribution and are a significant contribution to the total number of submicron particles. However, they hardly make any contribution to the total surface area or total volume of submicron particles. This tendency was seen every month from August to December. Ito and Iwai (1981) pointed out the possibility of photochemical production of particles smaller than 10^{-6} cm in radius in the Antarctic troposphere, based on the analyses of events with sudden increases in Aitken particle concentration. In this sense, the radius subrange smaller than 10^{-6} cm may be called a new particle subrange.

Particles larger than 10^{-5} cm in radius contrast with those in the new particle subrange. They make little contribution to the total number, but a significant contribution to the total surface area and total volume of submicron particles. This subrange mainly contains "large particles". In September when "large particles" reach their maximum concentration for the year, Syowa station frequently experienced storms which brought warm moist maritime air, containing a lot of sea salt particles (Ito, 1985). In this sense, the

radius subrange larger than 10^{-5} cm may be called a maritime subrange.

Particles with radii between 10^{-6} and 10^{-5} cm make a significant contribution to the total number, total surface area, and total volume of submicron particles. Particles in this subrange have a relatively long residence time and consist mainly of aged particles that are observed widely in the global background troposphere. In this sense, the subrange between 10^{-6} and 10^{-5} cm in radius may be called a background subrange.

The seasonal variation of size distribution was discussed by Ito (1985) using Fig. 5 and the results of the year-round observation of the mean size of Aitken particles. As a result of the discussion, it is speculated that for the seasonal variation of size distribution, a monomodal distribution with a mode in the background subrange prevails in the polar night months and a bimodal size distribution prevails in the sunlit months. In the early part of the sunlit months following the polar night months, the size distribution changes from monomodal to bimodal. Thereafter, the particle concentration of the new particle subrange soon saturates and tends to maintain a constant level, whereas the concentration in the background subrange increases from spring to summer.

Shaw (1980) made a measurement of solar aureole at the South Pole and found that the average size distribution of particles in the vertical air column over Antarctica had a bimodal shape with modes in the new particle subrange and the maritime subrange, respectively. At Ross Island, the size distribution of Aitken particles in the Antarctic continental air was bimodal with modes in the new particle subrange and the maritime subrange, whereas those in maritime air were bimodal with modes in the background subrange and maritime subranges (Shaw, 1986). The mode in the maritime subrange observed by Shaw may be thought unrealistic based on the observations at Syowa station.

The prevalence of a monomodal size distribution has been reported by Jaenicke et al. (1992) based on the 167 size distributions observed at Georg von Neumayer station, showing a monomodal distribution with a mode in the new particle subrange although the mode radius varies seasonally, that is, small in summer and large in winter.

Three types of size distribution have been reported from Mawson station based on 15 pairs of observed size distributions, that is, a monomodal size distribution with a mode in the new particle subrange, a monomodal size distribution with a mode in the background subrange and a bimodal size distribution with modes in the new particle and background subranges (Gras and Adriaansen, 1985). These three types appeared systematically at Mawson depending on the seasons; the monomodal distribution with a mode in the background subrange in winter, the monomodal distribution with a mode in the new particle subrange in summer, and the bimodal distribution in spring and fall (Gras, 1991; personal communication).

Although the differences in size distributions reported by different researchers seem to be attributed partly to the reliability of their observation methods, they may be consistent with each other if a different state of mixing of air masses with a characteristic aerosol size distributions in different locations and in different seasons is considered.

Fig. 6 illustrates the speculated characterization of size distribution in the atmospheric regimes over and around Antarctica, incorporated with the illustrations indicating the various atmospheric processes relating to the Antarctic aerosols given by Ito (1989). The size distributions are drawn in the four squares with grids. The scales of radius and concentration of size distributions are indicated only for the left-most square and the same applies to the others. For the size distributions, the solid curves indicate the size distribution in summer and the dashed curves represent winter.

The size distribution of aerosols in the Antarctic free atmosphere (AFA) is speculated to be monomodal with a mode in the new particle subrange in summer as suggested by Shaw (1986), Gras (1991, personal communication) and Jaenicke et al. (1992). In winter, the monomodal size distribution with a mode in the background subrange would be expected as suggested by Gras (1991, personal communication).

The size distribution of aerosols in the maritime free atmosphere (MFA) seems to have the same properties as that in the southern hemisphere background troposphere, assuming that the aerosols are aged and of monomodal size distribution with a mode in the background subrange in summer and in winter. The mode radius would be smaller in summer than in winter, assuming a

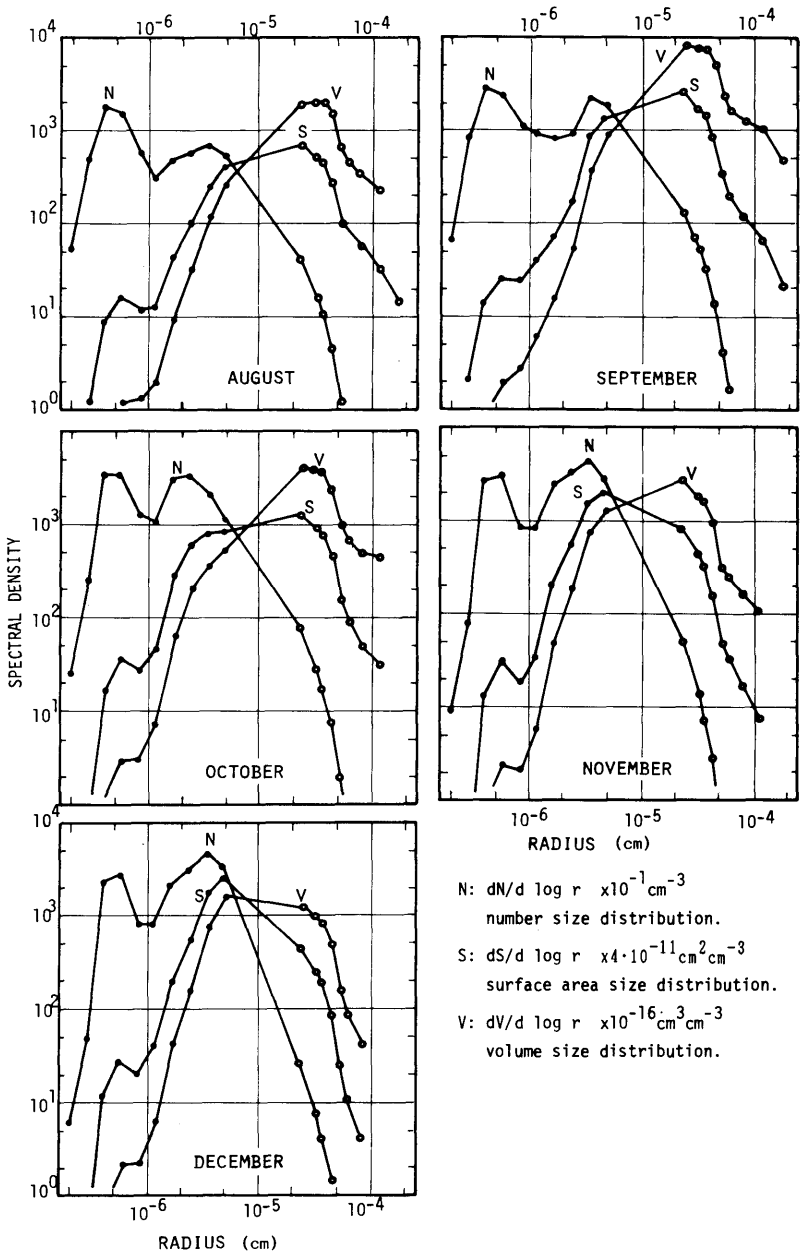

Fig. 5. Monthly average size distributions.

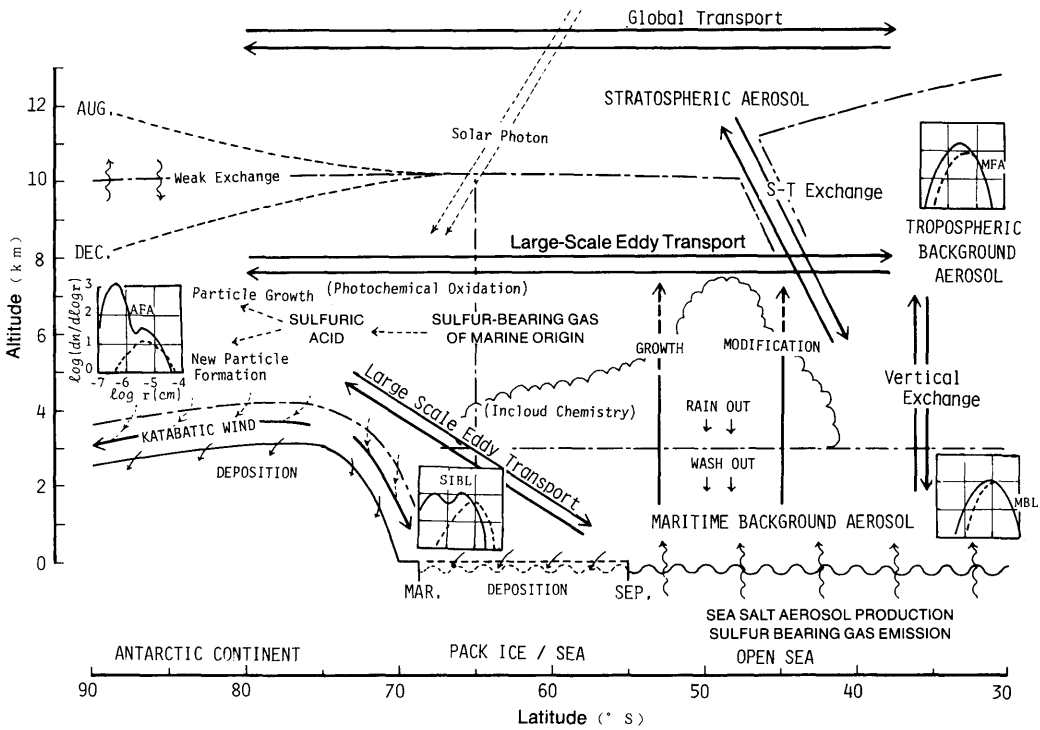

Fig. 6. The characterization of size distribution submicron aerosols in the atmospheric regimes over and around Antarctica. Details in the text. The illustration indicating the various atmospheric processes relating to the Antarctic aerosols is given by Ito (1989).

seasonality of new particle production rate similar to that suggested by Bigg et al. (1984).

The size distribution of aerosols in the maritime boundary layer (MBL) is speculated to be monomodal with a mode in the background subrange in summer as suggested by Shaw (1986) and also in winter. The mode radius would be larger and less seasonally variable than the MFA, assuming the high growth rate of aerosol by heterogeneous conversion of SO_2, dimethylsulfide (DMS), etc. in the MBL, as will be discussed later.

Since the boundary layer over the sea ice region (SIBL), as at Syowa station, is the intermediate between the AFA and MBL, the size distribution in the SIBL is speculated to comprise a mixture of the properties of aerosols in the MBL, MFA and AFA, resulting in the prevalence of a bimodal size distribution.

4.2. *Production rate of new particles expected from the observed size distribution*

The size distribution with a trough at around 10^{-6} cm in radius observed at Syowa station cannot be explained by the mechanism of in-cloud growth of cloud condensation nuclei as proposed by Hoppel et al. (1990) which tends to produce a trough at around 4×10^{-6} cm in radius. According to the numerical simulation by Walter (1973), the bimodal size distribution can exist persistently under the continuous production in the new particle subrange. In order to maintain the mode of the bimodal size distribution observed at Syowa station in the new particle subrange, continuous production of new particles is required, competing with the loss of new particles due to coagulation to existing particles. The residence time (or time constant of decay due to coagulation loss) of new particles can be estimated from the loss rate of the new particles by coagulation with the existing particles. Ignoring the time variation of size distribution, the residence time of new particles is estimated by

$$T_c \approx \left\{ \int_0^\infty K(r_0, r)\, f(r)\, \mathrm{d}r \right\}^{-1}, \qquad (2)$$

where T_c is the residence time of new particles with a radius of r_0, $f(r) = dn/dr$ is a size distribution of existing aerosols, $K(r_0, r)$ is the collision probability between particles with radii of r_0 and $r \cdot K(r_0, r)$ can be evaluated, for example, using the table given by Fuchs (1964). The production rate of new particles required to maintain the concentration in the new particle subrange competing with coagulation loss is estimated by

$$J_n \approx N_n / T_c, \tag{3}$$

where J_n is the production rate of new particles and N_n is the particle concentration in the new particle subrange. When the size distribution obtained in December as shown in Fig. 5 is used for $f(r)$, a value for $T_c = 2.6 \times 10^5$ s is obtained for $r_0 = 5 \times 10^{-7}$ cm. In the size distribution, the total concentration is approximately 450 cm^{-3}, and the concentration of particles in the new particle subrange is approximately 100 cm^{-3}. Then from eq. (3) the production rate of new particles required to maintain the concentration of $N_n = 100\ cm^{-3}$ in the new particle subrange is determined as $J_n \approx 3.8 \times 10^{-4}\ cm^{-3}\ s^{-1}$.

4.3. *Possible processes leading to new particle formation*

Recently, the submicron particles were collected at Asuka station (71°32′S, 24°08′E) during the period from January to December in 1988 with an electrostatic precipitator and were examined and sized for the particles of radii between 1.6×10^{-6} and 1.6×10^{-5} cm with an electron-microscope. The particles identified as sulfuric acid particles from their morphology prevailed in sunlit months and their size distribution was comparable to the part in the background subrange of size distribution shown in Fig. 6 (Okada et al., 1990). Existence of sulfuric acid in Antarctic submicron aerosols was confirmed by a more specific method using the thin film chemical test for the particles collected around Syowa station (Yamato et al., 1987).

The phenomenological behavior of submicron aerosols as summarized by Ito (1985, 1989) can be recognized as being closely correlated with each other, when we assume the production and growth of particles by condensation of sulfuric acid vapor which is produced photochemically within the Antarctic troposphere. The marked seasonal variation of solar irradiance in Antarctica might cause a large seasonal variation of the production rate of sulfuric acid vapor, producing in turn a seasonal variation of the production rate of new particles and the growth of existing particles. This may produce a seasonal variation of size distribution, concentration, and substances of submicron aerosols observed at Syowa station.

In the following part, the production of new particles in the Antarctic atmosphere will be examined by applying the existing nucleation theory for binary system of sulfuric acid and water. Fig. 7 indicates the flow chart of the following discussion.

4.3.1. Partial pressure of sulfuric acid vapor required to sustain the nucleation rate. As already explained, the persistence of the observed bimodal size distribution requires the continuous production of new particles with a radius of around 5×10^{-7} cm and a rate of $3.8 \times 10^{-4}\ cm^{-3}\ s^{-1}$ or more. The new particles are first created as critical embryos, aggregations of hundreds of molecules,

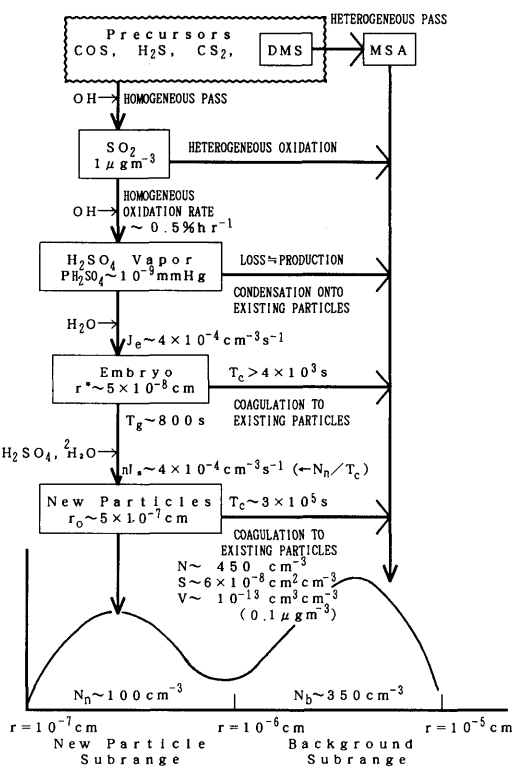

Fig. 7. Schematic diagram explaining possible processes of new particle formation in the Antarctic troposphere.

and then condensationally grow in size to form new particles with a radius of 5×10^{-7} cm. According to the numerical calculation in a monomer model by Mirabel and Katz (1974), the embryo production rate of $J_e = 10^{-4}$ cm^{-3} s^{-1} is attained under the condition of 50% relative humidity and 2×10^{-7} mmHg partial pressure of sulfuric acid ($P_{H_2SO_4}$). Suzuki and Mohnen (1981) claim that the binary system of sulfuric acid and water usually contains many polymers in hydrated forms. If the effect of hydrations is taken into account, the embryo production rate of $J_e = 10^{-4}$ cm^{-3} s^{-1} requires a rather higher $P_{H_2SO_4}$, say 5×10^{-7} mmHg at 50% relative humidity. Both theories, however, show that the same J_e can be attained by a lower $P_{H_2SO_4}$ under the condition of a higher relative humidity. For example in the monomer model, $P_{H_2SO_4}$ required to attain $J_e = 10^{-4}$ cm^{-3} s^{-1} at the relative humidity close to 100% is of the order of 10^{-9} mmHg at 25°C (Kreidenweis and Seinfeld, 1988). A relative humidity higher than 50% is attainable with an upward motion of air even over Antarctica.

Because the partial pressure of H_2SO_4 vapor over acid solutions decreases with a decrease in temperature (e.g., Jaecker-Voirol et al., 1990), the saturation ratio of H_2SO_4 vapor with the fixed vapor pressure in the ambient air increases with a decrease in temperature. The nucleation rate increases with an increase in the saturation ratio of H_2SO_4 vapor. It means the low temperature enhances the embryo production as demonstrated by Hegg et al. (1990). Thus, the Antarctic troposphere of low temperature can be expected possibly to have a higher nucleation rate, with the H_2SO_4 vapor pressure as low as 10^{-9} mmHg, than an atmosphere at 25°C.

Additional effects which enhance embryo production are also expected to be found in Antarctica. For instance, it is possible that in the case of the ternary system containing the third trace substances such as HNO_3 or NH_3OH, the nucleation rate is larger with the same value of $P_{H_2SO_4}$ comparing with a binary system (Ohta, 1982). It was confirmed that the submicron aerosols around Syowa station contained $(NH_3)_2SO_4$ (Yamato et al., 1991; personal communication) and HNO_3 (Yamato et al., 1991; Kanamori et al., 1991; personal communications). Therefore, embryo formation in Antarctica possibly proceeds in the ternary system or a more heteromolecular system which requires a much lower $P_{H_2SO_4}$ value to compare with binary system.

Highly aggregated ions consisting of more than 100 atoms have been detected in the troposphere (e.g., Heitmann and Arnold, 1983). In the polar region, ion productivity by cosmic ray is expected to be higher than in lower latitudes. If such highly aggregated to be higher than in lower latitudes. If such highly aggregated ions exist also in the Antarctic troposphere, they are possibly involved in nucleation processes which are enhancing the new particle production with a much lower $P_{H_2SO_4}$ value.

Taking these possibilities into account, it is reasonable to consider that the sulfuric acid vapor pressure of $P_{H_2SO_4} = 10^{-9}$ mmHg is enough to produce critical embryos at a rate of more than $J_e = 3.8 \times 10^{-4}$ cm^{-3} s^{-1}.

4.3.2. Stability of new embryos against their coagulation loss. The size of the critical embryos can be assumed as $r^* = 5 \times 10^{-8}$ cm in radii. During the growth of critical embryos to new particles, the embryos may decrease in concentration due to their coagulation with existing particles. The relative significance of this coagulation loss effect can be evaluated by comparing the time scale required for growth, and the residence time of the embryos limited by the coagulation loss rate.

At first, the estimation of the time scale required for the growth of critical embryos to new particles will be discussed. Since the concentration of H_2SO_4 molecules is much lower than that of H_2O, the impinging rate of H_2SO_4 molecules to an embryo is much lower than that of H_2O molecules. After one H_2SO_4 molecule impinges, many H_2O molecules impinge and evaporate until another H_2SO_4 impinges the embryo. It can be assumed that for normal relative humidity conditions an embryo captures up to 9 H_2O molecules for one captured H_2SO_4 molecule (Staufer et al., 1973). Then, the growth rate of embryos is approximated as

$$dr/dt \approx 10vBN_{H_2SO_4}, \tag{4}$$

where $v = 3 \times 10^{-23}$ cm^3 is the molecular volume of water and $B = \sqrt{kT/2\pi m} = 6 \times 10^3$ cm^{-3} s^{-1} ($k = 1.38 \times 10^{-23}$ J K^{-1} is the Boltzman constant; $T = 273$ K is the temperature; $m = 1.63 \times 10^{-22}$ g is the molecular mass of H_2SO_4). $N_{H_2SO_4}$ is the

number of sulfuric acid molecules in 1 cm^3 of air and is estimated by

$$N_{H_2SO_4} \approx N_L P_{H_2SO_4}/760, \quad (5)$$

where $N_L = 2.7 \times 10^{19}$ molecules cm^{-3} is the Loschmidt Number. The time required for the growth of an embryo from the size of r^* to r, that is, growth time T_g, is obtained by integrating eq. (4) as

$$T_g \approx (r - r^*)/10vBN_{H_2SO_4}. \quad (6)$$

When $P_{H_2SO_4} = 10^{-9}$ mmHg, then $N_{H_2SO_4} = 3.5 \times 10^7$ molecules cm^{-3}, so that T_g becomes about 800 s for the growth from $r^* = 5 \times 10^{-8}$ cm to $r = 10^{-7}$ cm, about 1.6×10^3 s from $r = 10^{-7}$ to $r = 2 \times 10^{-7}$ cm and about 4.8×10^3 s from $r = 2 \times 10^{-7}$ to $r_0 = 5 \times 10^{-7}$ cm.

The critical embryos have a residence time limited by the loss of embryos due to the coagulation to existing particles. For the existing aerosols having the same size distribution observed at Syowa station in December (Fig. 5), the residence time of small particles due to coagulation loss is calculated by an equation similar to eq. (2) as 2.6×10^5 s for $r = 5 \times 10^{-7}$ cm, 6.1×10^4 s for $r = 2 \times 10^{-7}$ cm, and 1.5×10^4 s for $r = 1 \times 10^7$ cm. From the extrapolation of these values, the residence time of critical embryos against coagulation losses can be estimated as the order of 4×10^3 s for the radius of $r^* = 5 \times 10^{-8}$ cm and it would become longer with an increase in size. This means that the residence time of growing embryos is expected to be nearly one order larger than the growing time T_g, suggesting that the loss of embryos during their growth from 5×10^{-8} to 5×10^{-7} cm is insignificant and that it is safe to consider $J_n \approx J_e$. Therefore, the embryo production rate of $J_e = 3.8 \times 10^{-4}$ cm^{-3} s^{-1} is considered to be sufficient for producing new particles to maintain the observed bimodal size distribution.

4.3.3. Conversion rate of SO_2 to H_2SO_4 and appropriate SO_2 concentration taking account of the H_2SO_4 loss to existing aerosols. The embryo production rate of $J_e = 3.8 \times 10^{-4}$ cm^{-3} s^{-1} requires the continuous production of H_2SO_4 vapor to maintain its vapor pressure at more than 10^{-9} mmHg, competing with the consumption of the H_2SO_4 vapor due to the condensation on existing particles. Sulfuric acid vapor in the atmosphere is produced through homogeneous (i.e., gas phase) photochemical oxidation of SO_2 but not through heterogeneous processes (i.e., on particles).

Only a few measurements of SO_2 concentration have been made in the Antarctic atmosphere. Cadle et al. (1968) reported that the concentration at McMurdo station varied from less than 0.5 to 1.6 ppbv (<1.4 to 4.6 $\mu g\, m^{-3}$ in the standard atmospheric temperature and pressure; STP). Molski et al. (1981) reported values ranging from 1.4 to 3.3 $\mu g\, m^{-3}$ at Arktowski station. Berresheim (1987) and Pszenny et al. (1989) reported much lower values ranging from 11 to 35 $ng\, m^{-3}$ in autumn over the Antarctic Ocean. In Southern Ocean regions, Nguyen et al. (1983) reported values of 0.25 $\mu g\, m^{-3}$ in December. Values reported by different researchers show considerable difference. The highest values may have suffered from local contamination. The lowest values may only be representative in the marine boundary layer where the heterogeneous oxidation of SO_2 is active (Pszenny et al., 1989; Luria and Sievering, 1991).

The homogeneous conversion rate of SO_2 required to produce H_2SO_4 vapor in the Antarctic troposphere is not known. In the remote oceanic regions, a conversion rate of 1.0–4.0% hr^{-1} has been determined (Ito et al., 1986; Bonsang et al., 1987). According to Luria and Sievering (1991), about 60% of the observed conversion in the marine boundary layer should occur via the heterogeneous channels, and the 24-h average homogeneous rate was reported to be approximately 1% hr^{-1}.

Assuming the SO_2 concentration is 1 $\mu g\, m^{-3}$ and the conversion rate is 0.5% hr^{-1}, the production rate of H_2SO_4 is estimated as $C_{H_2SO_4} = 1.3 \times 10^4$ molecules cm^{-3} s^{-1}. All of the H_2SO_4 vapor thus produced is not necessarily available for the production of embryos, but is consumed predominantly by the condensation on existing particles (Staufer et al., 1973). In steady state of the production and consumption of H_2SO_4 vapor, the partial pressure of sulfuric acid can be estimated by

$$P_{H_2SO_4} \approx 760 C_{H_2SO_4}/BSN_L \quad \text{mmHg}, \quad (7)$$

where S is the total surface area of existing particles in an air volume of 1 cm^3. The total surface area was estimated as 6×10^{-8} cm^2 cm^{-3} from the size distribution in December in Fig. 5. Then the

partial pressure was estimated as $P_{H_2SO_4} = 10^{-9}$ mmHg which is comparable to the value required for the production of embryos at a rate of 3.8×10^{-4} cm^{-3} s^{-1}.

Taking this into consideration, it is reasonable to predict that the new particle production with a rate sufficient to maintain the observed bimodal size distribution could possibly occur at Syowa station if an SO_2 concentration of 1 μg m^{-3} and a homogeneous conversion rate of 0.5% hr^{-1} is attained. In the case of an SO_2 concentration of 0.5 μg m^{-3}, the same result is produced for a conversion rate of 1% hr^{-1}.

4.3.4. Sources of SO_2 and the role of dimethylsulfide. Since the residence time of SO_2 is less than 30 hr (Ito et al., 1986; Bonsang et al., 1987) in the marine boundary layer and a few days in the free troposphere assuming only homogeneous conversion, SO_2 consumed through the conversion to H_2SO_4 in the Antarctic troposphere cannot be balanced by long-range transport from anthropogenic sources. Dimethylsulfide (DMS) emitted from the ocean may be a promising source of SO_2. Oxidation of DMS through the reaction with OH or NO_3 produces SO_2, methanesulfonate (MSA) etc. with a temperature dependency. In the cold polar region, the yield of SO_2 from DMS seems to be small compared with warm lower latitudes. This is supported by the observations indicating the large latitudinal gradient of the molar ratio of MSA and non-sea-salt (n.s.s.) sulfate in aerosols (e.g., Koga et al., 1991), although the seasonal variation of the ratio at Cape Grim, Tasmania reported by Ayers et al. (1991) gives the opposite figure for the temperature dependence. Ayers et al. (1991), Ayers and Gras (1991) and Hegg et al. (1991) reported the observational results suggesting that cloud condensation nuclei, n.s.s. sulfate, and MSA concentrations are strongly coupled to DMS. These reports, however, are still insufficient in giving evidence to regard DMS as a major precursor of SO_2, because the reported coherence between aerosol and DMS can be explained by the heterogeneous processes. Furthermore in the maritime boundary layer, quite low concentration of SO_2 has been observed (Berresheim, 1987) due to the effective oxidation of SO_2 through heterogeneous processes which do not produce H_2SO_4 vapor.

Thus for new particle formation from H_2SO_4 in the Antarctic troposphere, DMS in the lower troposphere is not such a promising precursor of SO_2. The source of H_2SO_4 vapor for the new particle formation in Antarctica should be searched for in the free troposphere. The layer with a high concentration of Aitken particles was detected over Antarctica through the observations with a balloon and airplane (Ito, 1989). The presence of a high concentration layer aloft might suggest that new particle production occurred in this layer and mixed into the boundary layer.

SO_2 measurements from an aircraft (Maroulis et al., 1980) show that the concentration in the free atmosphere is higher than in the boundary layer in both hemispheres. SO_2 in the free troposphere between 50°S and 60°S was about 100 pptv (0.3 μg m^{-3} STP) and increased towards high latitudes. Georgii and Meixner (1980) reported that an SO_2 concentration of about 500 pptv (1.4 μg m^{-3} STP) was representative above 6 km in the Northern Hemisphere. Their value was a few times higher than that in the Northern Hemisphere reported by Maroulis et al. (1980).

Shaw (1980) considered that SO_2 in the Antarctic troposphere is possibly balanced by the conversion from long-lived precursor gases such as CS_2 and COS. These gases are converted to SO_2 through the reaction with OH. Torres et al. (1980) reported that the concentration of COS is quite uniform with the value of about 500 pptv throughout the free atmosphere and boundary layer in both hemispheres. This value is several times higher than the SO_2 concentration measured in the same flight by Maroulis et al. (1980). Rodhe and Isaksen (1980) made a model calculation on the chemical production of tropospheric SO_2 and concluded that neither natural emission of H_2S and DMS at the surface nor man-made emission of SO_2 seems to be able to explain the relatively high concentration of SO_2 observed in the middle and upper troposphere in both hemispheres, and so a relatively long-lived precursor must be involved as a source gas. These studies suggest that SO_2 in the Antarctic free troposphere is maintained by the conversion of rather inert gases such as COS, CS_2 and others.

4.3.5. Remarks. In Antarctica, the upward flux of short wave radiation reflected from the high albedo surface snow and ice possibly plays a significant role in the photochemical reaction producing SO_2. Additionally, in summer months

the solar radiation is available throughout the day in Antarctica. Therefore, it is expected that the conversion from precursors to SO_2 and homogeneous conversion from SO_2 to H_2SO_4 take place actively in the summer in Antarctica. Active photochemical depletion of tropospheric ozone in the summer in Antarctica discussed by Schnell et al. (1991) may support the present argument.

Since the number concentration of submicron aerosols at the South Pole is almost half of that at Syowa station in December (Ito, 1989), the total surface area of existing aerosols in the Antarctic free troposphere is expected to be much smaller than those at Syowa station. This would provide more SO_2 and H_2SO_4 vapor for the new particle formation, because of fewer competing heterogeneous processes.

Taking two main factors characteristic in the summer Antarctic troposphere into account, that is, the small total surface area of existing particles and the high surface albedo in conjunction with long daytime duration, the concentration and conversion rate of SO_2 assigned in the present discussion seem to be reasonable and/or high $P_{H_2SO_4}$ can be expected even where the SO_2 concentration is lower than 1 $\mu g\,m^{-3}$. DMS emitted into the free atmosphere over the Antarctic ocean may be an additional precursor of SO_2 in the Antarctic free troposphere.

The composition of particles in the background subrange in Antarctica has been identified as predominantly H_2SO_4 by various researchers, but those in the new particle subrange have not yet been determined. The only information relating to the substances of particles in the new particle subrange came from volatility measurements which suggest that particles with similar volatility to sulfate, nitrate and organic substances prevailed in the new particle subrange in the summer in Antarctica (Ito, 1985). In this paper, the process of new particle formation is discussed under the assumption that the new particles are composed of sulfuric acid. However, Went (1966) and Jaenicke (1978) report that there is a significant amount of organic materials in Aitken particles. MSA vapor from DMS may also produce new particles. Little is known about these possibilities. Nucleation of substances other than sulfate would cause this to proceed along different lines than what is presented here.

5. Conclusion

New particle formation in the troposphere over remote regions is a key process which should be clarified to evaluate the possible role of aerosols in the climatic change as hypothesized by Charlson et al. (1987). The bimodal size distribution of submicron aerosols observed at Syowa station gives evidence of new particle formation in the Antarctic troposphere. The main factors enhancing the new particle production in the summer in Antarctica may be the small total surface area of existing particles and the high surface albedo in conjunction with long day-time duration.

Based on simplified theoretical calculations, it is concluded that the production rate of new particles is about $4 \times 10^{-4}\,cm^{-3}\,s^{-1}$ in the summer in Antarctica which would be yielded, for instance, by homogeneous conversion of an SO_2 concentration of 1 $\mu g\,m^{-3}$ at a rate of 0.5 % h^{-1}. The most plausible precursors of SO_2 involved in this process seem to be rather inert gases such as COS, CS_2 etc. DMS would have a small role in this new particle formation process in the Antarctic troposphere because it is thought to be consumed predominantly in the growth processes of existing particles in the marine boundary layer, even though Antarctica is surrounded by the oceanic region actively emitting large amount of DMS. However, in terms of aerosol mass, those converted from DMS would be of the most important sulfur species in Antarctica.

REFERENCES

Ayers, G. P., Ivey, J. P. and Gillett, R. W. 1991. Coherence between seasonal cycles of dimethyl sulphide, methanesulphonate and sulphate in marine air. *Nature 349*, 404–406.

Ayers, G. P. and Gras, J. L. 1991. Seasonal relationship between cloud condensation nuclei and aerosol methanesulphonate in marine air. *Nature 353*, 834–835.

Berresheim, H. 1987. Biogenic sulfur emissions from the Subantarctic and Antarctic oceans. *J. Geophys. Res. 92*, 13245–13262.

Bigg, E. K., Gras, J. L. and Evans, C. 1984. Origin of Aitken particles in remote region of the Southern Hemisphere. *J. Atmosph. Chem. 1*, 203–214.

Bonsang, B., Nguyen, B. C. and Lambert, G. 1987. Comment on "The residence time of aerosols and SO_2 in the long-range transport over the ocean", by Ito et al. *J. Atmosph. Chem. 5*, 367–369.

Cadle, R. D., Fischer, W. H., Frank, E. R. and Lodge, P. J. Jr. 1968. Particles in the Antarctic atmosphere. *J. Atmosph. Sci. 25*, 100–103.

Charlson, R. J., Lovelock, J. E., Andreae, M. O. and Warren, S. G. 1987. Oceanic phytoplankton, atmospheric sulfur, cloud albedo and climate. *Nature 326*, 655–661.

Davies, C. N. 1973. Diffusion and sedimentation of aerosol particles from Poiseuille flow in pipes. *Aerosol Sci. 4*, 317–328.

Fuchs, N. A. 1964. *The mechanics of aerosols.* Pergamon Press, 408 p.

Georgii, H. W. and Meixner, F. X. 1980. Measurement of the tropospheric and stratospheric SO_2 distribution. *J. Geophys. Res. 85*, 7433–7438.

Gras, J. L. and Adriaansen, A. 1985. Concentration and size variation of condensation nuclei at Mawson, Antarctica. *J. Atmos. Chem. 3*, 93–106.

Hegg, D. A., Radke, L. F. and Hobbs, P. V. 1990. Particle production associated with marine clouds. *J. Geophys. Res. 95*, 13917–13926.

Hegg, D. A., Ferek, R. J., Hobbs, P. V. and Radke, L. F. 1991. Dimethyl sulfide and cloud condensation nucleus correlations in the northeast Pacific ocean. *J. Geophys. Res. 96*, 13189–13191.

Heitmann, H. and Arnold, F. 1983. Composition measurements of tropospheric ions. *Nature 306*, 747–751.

Hogan, A. W. 1975. Antarctic aerosols. *J. Appl. Meteorol. 14*, 550–559.

Hoppel, W. A., Fitzgerald, J. W., Frick, G. M. and Larson, R. E. 1990. Aerosol size distributions and optical properties found in the marine boundary layer over the Atlantic ocean. *J. Geophys. Res. 95*, 3659–3686.

Ito, T. 1976. An automatic Pollak counter improved for routine field operation. *J. Meteor. Soc. Japan 54*, 81–90.

Ito, T. 1980. On the size distribution of submicron aerosols in the North Pacific air. *J. Meteor. Soc. Japan 58*, 81–92.

Ito, T. 1982. On the size distribution of submicron aerosols in the Antarctic atmosphere. *Antarctic Record, no. 76*, 1–19.

Ito, T. 1985. Study of background aerosols in the Antarctic troposphere. *J. Atmosph. Chem. 3*, 69–91.

Ito, T. 1989. Antarctic submicron aerosols and long-range transport of pollutants. *AMBIO 18*, 34–41.

Ito, T. and Iwai, K. 1981. On the sudden increase in the concentration of Aitken particles in the Antarctic atmosphere. *J. Meteor. Soc. Japan 59*, 262–271.

Ito, T., Okita, T., Ikegami, M. and Kanazawa, I. 1986. The characterization and distribution of aerosol and gaseous species in the winter monsoon over the western Pacific Ocean. II: The residence time of aerosols and SO_2 in the long-range transport over the ocean. *J. Atmos. Chem. 4*, 401–411.

Jaecker-Voirol, A., Ponche, J. L. and Mirabel, P. 1990. Vapor pressures in the ternary system water-nitric acid-sulfuric acid at low temperatures. *Journ. Geophys. Res. 95*, 11857–11863.

Jaenicke, R. 1978. The role of organic material in atmospheric aerosols. *Pageoph. 116*, 283–292.

Jaenicke, R., Dreiling, V., Lehmann, E., Koutsenogii, P. K. and Stingl, J. 1992. Condensation nuclei at the German Antarctic station Georg von Neumayer. *Tellus 44B*, 311–317.

Koga, S., Tanaka, H., Yamato, M., Yamanouchi, T., Nisio, F. and Iwasaka, Y. 1991. Methanesulfonic acid and non-sea-salt sulfate over both hemispheric Oceans. *J. Meteorol. Soc. Japan 69*, 1–14.

Kreidenweis, S. M. and Seinfeld, J. 1988. Nucleation of sulfuric acid-water and Methanesulfonic acid-water solution particles: Implications for the atmospheric chemistry of organosulfur species. *Atmos. Environ. 22*, 283–296.

Luria, M. and Sievering, H. 1991. Heterogeneous and homogeneous oxidation of SO_2 in the remote marine atmosphere. *Atoms. Environ. 25A*, 1489–1496.

Maroulis, P. J., Torres, A. L., Goldberg, A. B. and Bandy, A. R. 1980. Atmospheric SO_2 measurements on project GAMETAG. *J. Geophys. Res. 85*, 7345–7349.

Mirabel, P. and Katz, J. L. 1974. Binary homogeneous nucleation as a mechanism for the formation of aerosols. *J. Chem. Phys. 60*, 1138–1144.

Molski, B., Bytnerowicz, A. and Dmuchowski, W. 1981. Air pollution with sulfur dioxide and fluorine compounds in the vicinity of the Arctowski Station, King George Island, South Shetland Islands. *Pol. Polar Res.* 2 (1–2), 87–93, 1981.

Nguyen, B. C., Bonsang, B. and Gaudry, A. 1983. The role of the ocean in the global atmospheric sulfur cycle. *J. Geophys. Res. 88*, 10903–10914.

Ohta, S. 1982. On the rate of homogeneous nucleation in ternary systems. *J. Aerosol. Sci. 13*, 139–145.

Okada, K., Aoki, T., Ikegami, M., Zaizen, Y. and Ito, T. 1990. Aitken sulfuric-acid particles in the Antarctic atmosphere. *Proc. of the 3rd International Aerosol Conference*, 24–27 September 1990, Kyoto Japan, 1132–1135.

Pszenny, A. A. P., Castelle, A. J., Galloway, J. N. and Duce, R. A. 1989. A study of the sulfur cycle in the Antarctic marine boundary layer. *J. Geophys. Res. 94*, 9818–9830.

Robinson, E., Bodhaine, B. A., Komhyr, W. D., Oltmans, S. J., Steele, L. P., Tans, P. and Thompson, T. M. 1988. Long-term air quality monitoring at the South Pole by

the NOAA program Geophysical Monitoring for Climatic Change. *Reviews of Giophysics 26*, 63–80.

Rodhe, H. and Isaksen, I. 1980. Global distribution of sulfur compounds in the troposphere estimated in a height/latitude transport model. *J. Geophys. Res. 85*, 7401–7409.

Schnell, R. C., Liu, S. C., Oltmans, S. J., Stone, R. S., Hofmann, D. J., Dutton, E. G., Deshler, T., Sturges, W. T., Harder, J. W., Sewell, S. D., Trainer, M. and Harris, J. M. 1991. Decrease of summer tropospheric ozone concentrations in Antarctica. *Nature 351*, 726–729.

Shaw, G. E. 1979. Considerations on the origin and properties of the Antarctic aerosol. *Rev. Geophys. Space Phys. 17*, 1983–1998.

Shaw, G. E. 1980. Optical, chemical and physical properties of aerosols over the Antarctic ice sheet. *Atmospheric Environ. 14*, 911–921.

Shaw, G. E. 1986. On physical properties of aerosol at Ross Island, Antarctica. *J. Aerosol Sci. 17*, 937–945.

Shaw, G. E. 1988. Antarctic aerosols: a review. *Reviews of Geophysics 26*, 89–112.

Staufer, D., Mohnen, V. A. and Kiang, C. S. 1973. Heteromolecular condensation theory applied to particle growth. *Aerosol Sci. 4*, 461–471.

Suzuki, K. and Mohnen, V. A. 1981. Binary homogeneous nucleation theory by cluster-cluster interaction with application to the H_2SO_4-H_2O system. *J. Aerosol Sci. 12*, 61–73.

Tan, C. W. and Hsu, C. J. 1971. Diffusion of aerosols in laminar flow in a cylindrical tube. *Aerosol Sci. 2*, 117–124.

Torres, A. L., Maroulis, P. J., Goldberg, A. B. and Bandy, A. R. 1980. Atmospheric OCS measurements on project GAMETAG. *J. Geophys. Res. 85*, 7357–7360.

Walter, H. 1973. Coagulation and size distribution of condensation aerosols. *Aerosol Sci. 4*, 1–5.

Went, F. W. 1966. On the nature of Aitken condensation nuclei. *Tellus 18*, 549–556.

Yamato, M., Iwasaka, Y., Tanaka, Okada, K., Ono, A., Nisio, F. and Fukabori, M. 1987. Evidence for the presence of submicron sulfuric acid particles in summer Antarctic Atmosphere: preliminary results. Proc. NIPR Symp. *Polar Meteorol. Glaciol. 1*, 74–81.